DIRECTIONAL MANIPULABILITY FOR MOTION COORDINATION OF AN ASSISTIVE MOBILE ARM

K. Nait-Chabane, P. Hoppenot, E. Colle
IBISC Université d'Evry Val d'Essonne, 40 rue de plevoux 91020, Evry, France
chabane@iup.univ-evry.fr , hoppenot@iup.univ-evry.fr, colle@iup.univ-evry.fr

Keywords: mobile manipulator, manipulability, redundancy systems, robotic assistance

Abstract: In this paper, we address the problem of coordinated motion control of a manipulator arm embarked on a mobile platform. The mobile manipulator is used in providing assistance for disabled people. In order to perform a given task by using mobile manipulator redundancy, we propose a new manipulability measure that incorporates both arm manipulation capacities and the end-effector imposed task. This proposed measure is used in a numerical algorithm to solve system redundancy and then compared with other existing measures. Simulation and real results show the benefit and efficiency of this measure in the field of motion coordination.

1 INTRODUCTION

In assistive robotics, a manipulator arm constitutes one possible solution for restoring some manipulation functions to victims of upper limb disabilities. The literature proposes three distinct manipulator arm configurations. The first one consists of a workstation in which a manipulator arm evolves within a structured environment (RAID, AFMASTER (Busnel, 2001)). According to the second configuration, a manipulator arm is added to an electrical wheelchair ((Kwee, 1993), (Evers, 2001)). The third configuration serves to expand the field of action for assistance systems; this configuration entails a mobile manipulator arm (MoVAR (Van der Loos, 1995), URMAD-MOVAID (Dario, 1999) and ARPH (Hoppenot, 2002)) that offers many advantages. Our research deals with this third configuration. Such a system however possesses more degrees of freedom than necessary for task execution. Any given point in the workspace may be reached by moving the manipulator arm or moving the mobile platform or by a combination of both. To facilitate the use of the system by the disabled person, the idea is that the operator pilots the gripper and that the remainder of the articulated system follows the movement of the gripper. We have focused attention on the use of redundancy for controlling a mobile arm.

Manipulability measures play an important role in the design, analysis, evaluation and optimization in manipulation robotics; it is a scalar that quantifies how well the system behaves with respect to force and motion transmission. These measures however do not include information either on the task imposed or on the direction of end-effector motion. We propose an additional measure that takes the task to be performed into account.

This paper is organized as follows. Section 2 presents the work conducted towards devising different solutions to the redundancy problem. Section 3 discusses the mobile arm and its kinematic models before Section 4 introduces the manipulability concept and primary set of related measures used in the literature on robotics. Section 5 then lays out a new measure that takes both the system manipulation capacities and task in progress into account. We will recall the principle behind the kinematic control scheme used to solve redundancy problems in Section 6, followed by an illustration of the benefit of our new measure by means of simulation and real results (in Section 7).

2 RELATED RESEARCH WORK

A considerable amount of interest has been shown over the past few years in mobile manipulators. Seraji (Seraji, 1993) presents a simple online approach for the motion control of mobile manipulators using augmented Jacobian matrices. This kinematic approach requires additional constraints to be satisfied for the manipulator configuration. The approach proposed may be applied with equal ease to both nonholonomic and holonomic mobile robots. Yamamoto and Yun (Yamamoto, 1987) set out to decompose the motion of the mobile manipulator into two subsystems based on the concept of preferred operating region. The mobile platform is controlled so as to bring the manipulator into a preferred operating region/configuration, with respect to the mobile platform, as the manipulator performs a variety of unknown manipulation tasks. The authors used the manipulability measure of the manipulator arm to define this preferred operating region. The principal advantage of this approach lies in its decentralized planning and control of the mobile platform and manipulator arm. However, the case when the manipulator is mounted at the center of the axis between the two driving wheels lies at a singularity in the method proposed by Yamamoto and Yun (Yamamoto, 1987). Nagatani (Nagatani, 2002) developed an approach to plan mobile base's path which satisfies manipulator's manipulability. The controllers used for manipulation and locomotion differ from one another.

Khatib (Khatib, 1995) Khatib [10] proposed to use a joint limit constraint in mobile manipulation in the form of potential function while his approach is to use the inherent dynamics characteristics of mobile manipulator in operational space. Additionally, he analyzed the inertial properties of a redundant arm with macro-micro structure. Kang (Kang, 2001) derived a combined potential function algorithm to determine a posture satisfying both the reduced inertia and joint limit constraints for a mobile manipulator. The author then integrated the inertia property algorithm into a damping controller in order to reduce the impulse force upon collision as well as to regulate contact.

Yoshikawa (Yoshikawa, 1990) introduced the arm manipulators manipulability and used it to solve the redundancy of such systems. The manipulability of mobile manipulator has been studied by few authors. Yamamoto and Yun (Yamamoto, 1999) have treated both locomotion and manipulation within the same framework from a task space perspective. They have presented the kinematic and dynamic contributions to manipulators and platforms by means of the so-called task space ellipsoid.

Bayle (Bayle, 2001) extended the definition of manipulability to the case of a mobile manipulator and then applied it in an inversion process for solving redundancy.

3 DESCRIPTION OF ROBOTIZED ASSISTANT

The mobile manipulator consists of a Manus arm mounted on a mobile platform powered by two independent drive wheels. Let's start by defining a fixed world reference frame $\{W\}$, a moving platform frame $\{P\}$ attached to the midway between the two drive wheels, a moving arm frame $\{A\}$ related to the manipulator base, and a moving end-effector frame $\{E\}$ attached to the arm end-effector (see Fig. 1).

We will adopt the following assumptions in modeling the mobile manipulator system: no slipping between wheel and floor; a platform incapable of moving sideways in order to maintain the nonholonomic constraint; and a manipulator rigidly mounted onto the platform.

The forward kinematics of a serial chain manipulator relating joint space and task space variables is expressed by:

$$X_a = f_a(q_a) \quad (1)$$

where $X_a = [x_{a1}, x_{a2}, \cdots x_{am}]^T \in R^m$ is the vector of task variables in an m-dimensional task space, $q_a = [q_{a1}, q_{a2}, \cdots q_{an}]^T \in R^n$ is the vector of joint variables in n-dimensional variables (called the generalized coordinates), and f_a is the nonlinear function of the forward kinematic mapping

$$\dot{X}_a = J_a(q_a)\dot{q}_a \quad (2)$$

where $\dot{X}_a$ is the task velocity vector, $\dot{q}_a$ the joint velocity vector and $J_a(q_a)$ the Jacobian matrix.

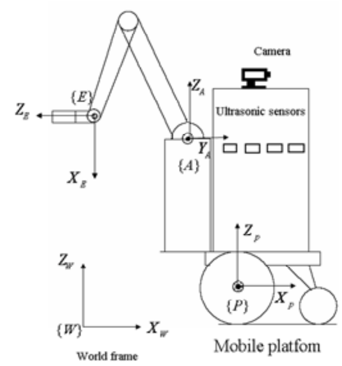

Figure 1: mobile manipulator system.

For the kinematic modeling of the considered manipulator arm, we make use of Denavit-Hartenberg parameters (Sciavicco, 1996). Manus arm possesses six rotoid joints, with 3 DOF for gripper positioning and 3 DOF for gripper orientation. The Cartesian coordinates of the end-effector relative to the arm base frame $\{A\}$ are given by:

$$X_a = \begin{cases} x_{a1} = (L_4 c_3 + L_3 c_2) c_1 - L_2 s_1 \\ x_{a2} = (L_4 c_3 + L_3 c_2) s_1 + L_2 c_1 \\ x_{a3} = L_4 s_3 + L_3 s_2 \\ x_{a4} = \phi \\ x_{a5} = \theta \\ x_{a6} = \psi \end{cases} \quad (3)$$

where $c_i = \cos(q_{ai})$, $s_i = \sin(q_{ai})$ and L_2, L_3, L_4 represent the length of shoulder, upper arm and lower arm, respectively.

$[x_{a1}, x_{a2}, x_{a3}]^T$ and $[\phi, \theta, \psi]^T$ represent the Cartesian coordinates and Euler angles of the end-effector, respectively. In this paper, we will only consider the three main joints of the arm, as given by the generalized vector $q_a = [q_{a1}, q_{a2}, q_{a3}]^T$.

The platform location is given by three operational coordinates x_p, y_p and θ_p, which define its position and orientation. The generalized coordinate vector is thus: $q_p = [x_p, y_p, q_p]^T$ and the generalized velocity vector is: $\dot{q}_p = [\dot{x}_p, \dot{y}_p, \dot{\theta}_p]$.

The constraint equation applied to the platform has the following form:

$$A(q_p)\dot{q}_p = 0 \quad (4)$$

in which $A(q_p) = [\sin(\theta_p) \;\; -\cos(\theta_p) \;\; 0]$.

The kinematic model of the mobile platform is given in (Campion, 1996):

$$\dot{q}_p = S(q_p) u_P \quad (5)$$

where $S(q_p) = \begin{bmatrix} \cos(\theta_p) & 0 \\ \sin(\theta_p) & 0 \\ 0 & 1 \end{bmatrix}$ and $u_p = [v, \omega]^T$, with v and ω being the linear and angular velocities of the platform, respectively.

The forward kinematic model of the mobile manipulator may be expressed in the following form:

$$X = f(q_p,\, q_a) \quad (6)$$

where q_p is the generalized coordinates of the mobile platform and q_a the joint variables of the arm, as defined above.

The configuration of the mobile manipulator is therefore defined by the N generalized coordinates ($N=n+3$):

$$q = [q_p^T, q_a^T]^T = [x_p, y_p, q_p, q_{a1}, \ldots, q_{an}]^T \quad (7)$$

The direct kinematic model for the positioning task of the considered mobile arm relative to world frame $\{W\}$ is given by:

$$X = [x_1, x_2, \cdots, x_6]^T = f(q_a, q_p) \quad (8)$$

$$X = \begin{cases} x_1 = x_p + (x_{a2} + a)\,c_{\theta_p} - (b - x_{a1})\,s_{\theta_p} \\ x_2 = y_p + (x_{a2} + a)\,s_{\theta_p} + (b - x_{a1})\,c_{\theta_p} \\ x_3 = x_{a3} + c \\ x_4 = x_{a4} + \theta_p - \frac{\pi}{2} = \phi + \theta_p - \frac{\pi}{2} \\ x_5 = x_{a5} = \theta \\ x_6 = x_{a6} = \psi \end{cases} \quad (9)$$

where $c_{\theta_p} = \cos(\theta_P)$, $s_{\theta_p} = \sin(\theta_P)$; a, b and c are the Cartesian coordinates of the manipulator arm base with respect to the mobile platform frame $\{P\}$.

The instantaneous kinematic model is then given by:

$$\dot{X} = J(q)\dot{q} \quad (10)$$

with: $J(q) = \frac{\partial f}{\partial q}$.

We can observe that generalized velocities $\dot{q}$ are dependent; they are linked by the nonholonomic constraint. The platform constraint described by (4) can be written in the following form:

$$[A(q_p) \;\; 0]\dot{q} = 0 \tag{11}$$

According to (5), the relation between the generalized velocity vector of the system and its control velocities can be written as follows:

$$\dot{q} = M(q)u \tag{12}$$

where $M(q) = \begin{bmatrix} S_p(q_p) & 0 \\ 0 & I_n \end{bmatrix}$.

I_n is an n-order identity matrix and $u = [v, w, \dot{q}_{a1}, \cdots, \dot{q}_{an}]^T$.

The instantaneous kinematic model does not include the nonholonomic constraint of the platform given by (11). The relationship between the operational velocities of the mobile manipulator and its control velocities takes the nonholonomic platform constraint into account and may be expressed by the reduced direct instantaneous kinematic model, i.e.:

$$\dot{X} = \bar{J}(q)u \tag{13}$$

with: $\bar{J}(q) = J(q)M(q)$.

4 MANIPULABILITY MEASURES

A well-established tool used for the motion analysis of manipulators is known as the manipulability ellipsoid approach. The concept of *manipulability* was originally introduced by Yoshikawa ((Yoshikawa, 1985), (Yoshikawa, 1990)) for arm manipulators, in order to denote a measure for the ability of a manipulator to move in certain directions. The set of all end-effector velocities that may be attained by joint velocities such that the Euclidean norm of $\dot{q}_a$, $\|\dot{q}_a\| = (\dot{q}_{a1}^2 + \dot{q}_{a2}^2 + \cdots \dot{q}_{an}^2)^{1/2}$, satisfying $\|\dot{q}_a\| \le 1$ is an ellipsoid in m-dimensional Euclidean space. This ellipsoid represents the manipulation capability and is called the "manipulability ellipsoid".

Yoshikawa defines the manipulability measure w as follows:

$$w = \sqrt{\det(J_a(q_a)J_a^T(q_a))} \tag{14}$$

which can be simplified into $w = |\det(J_a(q_a))|$ when $J_a(q_a)$ is a square matrix.

Let's now consider the singular value decomposition of J_a, as given by:

$$J_a = U_a \Sigma_a V_a^T \tag{15}$$

where $U_a \in R^{m\times m}$ and $V_a \in R^{n\times n}$ are orthogonal matrices, and:

$$\Sigma_a = \begin{bmatrix} \sigma_{a1} & & & 0 & \vdots & \\ & \sigma_{a2} & & & \vdots & \\ & & . & & \vdots & 0 \\ & & & . & \vdots & \\ 0 & & & \sigma_{am} & \vdots & \end{bmatrix} \in R^{m\times n} \tag{16}$$

in which: $\sigma_{a1} \ge \sigma_{a2} \ge \cdots \ge \sigma_{am}$.

The value of $w = \sigma_{a1}.\sigma_{a2}.\cdots\sigma_{am}$ is proportional to the ellipsoid volume.

Another measure has been proposed for characterizing the distance of a configuration from a singularity (Salisbury, 1982). This measure is given by:

$$w_2 = \frac{\sigma_{am}}{\sigma_{a1}} \tag{17}$$

where σ_{a_1} and σ_{a_m} are the maximum and minimum singular values of the Jacobian matrix, respectively.

Bayle (Bayle, 2001) defined a measure w_5 that extended the notion of eccentricity of the ellipse, i.e.:

$$w_5 = \sqrt{1 - \frac{\sigma_{am}^2}{\sigma_{a1}^2}}. \tag{18}$$

The structure of the manipulator arm consists of an arm portion with three joints and a wrist portion with three joints whose axes intersect at a single point. The arm portion concerns the positioning task, while the wrist portion focuses on gripper orientation. It proves quite useful to divide this study into wrist and arm singularities. We present herein the manipulability of the considered system for positioning tasks.

5 DIRECTIONAL MEASURE

All of the abovementioned measures describe system manipulability in general terms, without taking the task the manipulator is being asked to perform into account. One key factor behind the failure of these measures is the fact that they do not include information either on the task or on the direction the end-effector is required to move. A new measure should therefore be introduced to address this situation.

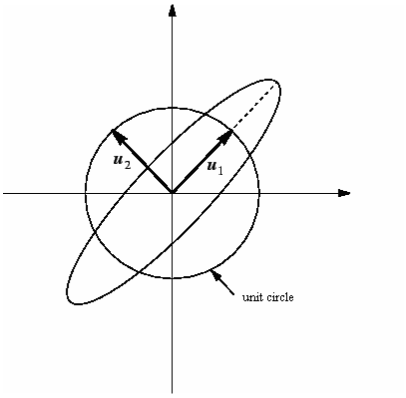

Figure 2: Manipulability ellipse in the two-dimensional case

The Singular Value Decomposition (15) of the Jacobian matrix and its geometric relationship offer further insights into characterizing the manipulability of mechanical systems. Let u_{ai} be the i^{th} column vector of U_a. The primary axes of the manipulability ellipsoid are then: $\sigma_{a1}u_{a1}, \sigma_{a2}u_{a2}, \cdots \sigma_{am}u_{am}$. Figure 2 provides an illustration of the two-dimensional case, according to which u_1 and u_2 yield the major and minor ellipse axes, respectively. We propose to include information on the direction of the task wished to precisely know the manipulation capacity of the arm manipulator for the execution of this operational task.

Let $\dot{X}_d$ be the desired task. We now define a unit vector $d = \frac{\dot{X}_d}{\left\|\dot{X}_d\right\|}$, which gives the direction of the imposed task.

By using properties of the scalar product and the singular values that represent radius of the ellipsoid, we define a new manipulability measure as being the sum of the absolute values of the scalar products of the directional vector of the task by the singular vectors pondered by their corresponding singular values. This new measure is noted w_{dir}.

$$w_{dir} = \sum_{i=1}^{m} \left| (d^T.u_{ai})\sigma_{ai} \right| \qquad (19)$$

This measure is maximized when the arm capacity of manipulation according to the direction of the task imposed is maximal. It is equal to zero if there is no possibility of displacement according to this direction.

6 CONTROL SCHEME

Whitney (Whitney, 1969) first proposed using the pseudo-inverse of the manipulator Jacobian in order to determine the minimum norm solution for the joint rates of a serial chain manipulator capable of yielding a desired end-effector velocity. A weighted pseudo-inverse solution approach also allows incorporating the various capabilities of different joints, as discussed in Nakamura (Nakamura, 1991) and Yoshikawa (Yoshikawa, 1984). One variant of this approach includes superposition of the Jacobian null space component on the minimum norm solution to optimize a secondary objective function (Baerlocher, 2001).

This same notion can then be extended to the case of a nonholonomic mobile manipulator. The inverse of the system given by equation (12) exhibits the following form:

$$u = \bar{J}^+ \dot{X}_d + (I - \bar{J}^+ \bar{J})Z \qquad (20)$$

where Z is a (N-1)-dimensional arbitrary vector.

The solution to this system is composed of both a specific solution $\bar{J}^+ \dot{X}_d$ that minimizes control velocities norm and a homogeneous solution $(I - \bar{J}^+ \bar{J})Z$ belonging to the null space $N(\bar{J})$. By definition, these latter added components do not affect task satisfaction and may be used for other purposes. For this reason, the null space is sometimes called the redundant space in robotics.

The Z vector can be utilized to locally minimize a scalar criterion. Along the same lines, Bayle (Bayle,2001b) proposed the following scheme:

$$u = \bar{J}^{+}\dot{X}_d - W(I - \bar{J}^{+}\bar{J})M^T\left(\frac{\partial P}{\partial q}\right)^T \qquad (21)$$

where $\dot{X}_d$ is the desired task vector, W a positive weighting matrix, and $P(q)$ the objective function dependent upon manipulator arm configuration. To compare the advantage of our manipulability measure with those presented in the literature, the control scheme whose objective function depends on various measures (w, w_5 and w_d) is to be applied. For manipulation tasks involving a manipulator arm, it is helpful to consider manipulability functions whose minima correspond to optimal configurations, e.g. ($-w$), ($-w_d$) or w_5.

As for the calculus, we used the numerical gradient of $P(q)$.

7 RESULTS

7.1 Simulation results

In this section, we will consider a Manus arm mounted on a nonholonomic mobile platform powered by two independent-drive wheels, as described in Section 3. The mobile platform is initially directed toward the positive X-axis at rest (q_p=[0, 0, 0]^T) and the initial configuration of the manipulator arm is: q_a= [4.71, 2.35, 4.19]^T (*rad*). The arm is fixed on the rear part of the platform. The coordinates of the arm base with respect to the platform frame are: [-0.12, -0.12, 0.4]^T (*m*). The imposed task consists of following a straight line along a Y-axis of the world frame {W}. The velocity along a path is constant and equal to 0.05 m.s^{-1}. Results obtained in the following cases have been reported:

- in optimizing arm manipulability measure w;
- in optimizing arm manipulability measure w_{dir}.

The comparison criteria are thus:

- Platform trajectory profile,
- indicator of energy spent E by the platform,
- manipulation capacity of the arm at the end of the task, measured by w.

w is the most widely used indicator of manipulability found in the literature. In our case, w serves as a reference to evaluate the efficiency of the control algorithm in terms of arm manipulability; its values range between 0, which corresponds to singular configurations, and 0.06, which corresponds to good manipulability. In addition, we are looking for forward displacements of the platform and smooth trajectories. End-effector trajectories enable checking if the task has been performed adequately.

E is defined by $E = \sum v_l^2 + v_r^2$, with v_l and v_r the linear velocities respectively of the left and right wheels of the platform.

Before presenting each case separately, it should be noted that, for each one of them, the task is carried out correctly.

Figure 3 shows simulation results in which arm manipulability w is used as the optimizing criterion for solving mobile arm redundancy. As depicted in Figure 3a, the arm manipulability w quickly improves up to a threshold corresponding to acceptable configurations. Around 25 seconds, local degradation of the manipulability measure is shown to be quite low.

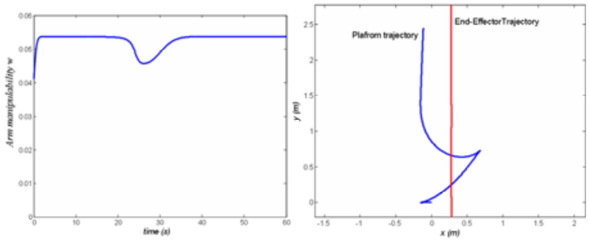

(a) (b)

Fig.3: Simulation result when optimizing arm manipulability measure w

To quickly improve arm manipulability while performing the imposed task, the arm extends and the platform retracts (see Fig. 3b). The platform stops retracting once arm manipulability has been optimized; afterwards, it advances so that the unit carries out the imposed task. This evolution corresponds to the first graining of the platform trajectory. Since the platform is poorly oriented with respect to the task direction, its contribution is limited by the nonholonomic constraint, which does cause slight degradation to the manipulability, as shown in Figure 3a. The reorientation of the platform, which corresponds to the second point of graining, allows for improvement and optimization of the manipulability measure. The mobile arm achieves the desired task with an acceptable arm configuration from a manipulation perspective; the platform moves in reverse gear however, which counters our intended aim. As there are two graining points, the platform trajectory is not smooth. The energy indicator E for this trajectory is $E=7.15m^2 s^{-2}$.

In Figure 4, we have used the proposed directional manipulability of the arm to solve mobile arm redundancy. Figure 4a shows the evolution of the directional manipulability measure w_{dir}, and arm manipulability w for comparison. The directional manipulability of the arm is initially good; it decreases slightly then improves progressively. Corresponding measure w does not reach its maximum value, but remains in a beach of acceptable values, far from the singular configurations. In this case, no local degradation of the manipulability measure is detected. Figure 4b presents the trajectory of the middle axis point on the platform. This figure indicates that the mobile platform retracts during a short period of time at the very beginning in order to improve arm manipulability. The platform reorients itself according to the imposed task without changing its motion direction. In executing a desired task, the platform thus follows a smoother trajectory and displays forward displacements. The energy indicator E for this trajectory is $E=3.1\ m^2.s^{-2}$. Energy expenditure is lower than the preceding case.

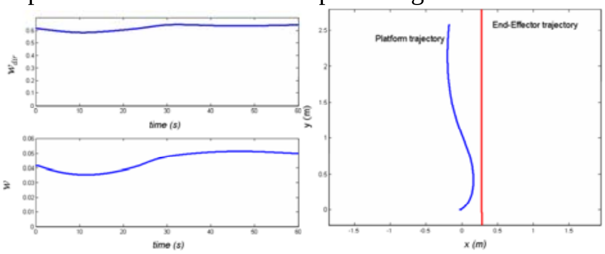

(a) (b)

Fig.4: Simulation result when optimizing arm directional manipulability measure w_{dir}

7.2 Results on real system

To illustrate the results presented in theory, we implemented on the real robot the algorithm. Starting from a given configuration q_i, collected by the sensors data, we impose an operational task on the end effector of the arm manipulator which consists in following a straight line according to the direction perpendicular to the axis longitudinal of the platform (Y axis of the world frame). Imposed velocity is 0.005 m per 60 ms cycle.

It should be noted that for each case, the task is carried out correctly with good configuration from manipulability point of view.

Figure 5 presents the platform and end effector trajectories respectively in the cases of optimizing arm manipulability w (figure 5a) and arm directional manipulability w_{dir} (figure 5b).

Platform and OT trajectories presented on Figure 5a show that the platform carries out most part of its movement in reverse gear. The end effector follows a straight line with an error which reaches 21 cm in end of the task. This error includes a set of measurement errors and the tracking error.

In the case of directional manipulability optimization, figure 5b indicates that the platform moves back a little at the beginning and moves according to the direction of the task. End-effector follows a straight line with a weak error at the beginning (less than 3cm) better than the case of the optimization of w. The tracking error increases at the end of the execution of the task. Indeed, as the calculation of the gripper position is done on the basis of odometric data, which generates not limited errors, the tracking error increases.

In both cases, the error level is tolerable for our application in which the user is active in the command loop.

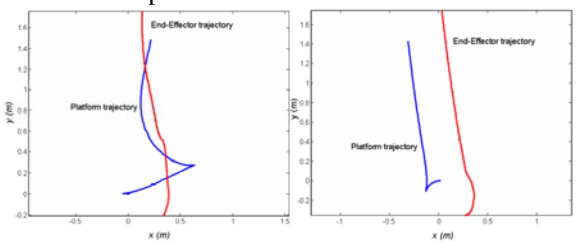

(a) (b)

Fig.5: End-Effector and platform trajectories in the real case

7.3 Discussion

For all the cases studied, the task has been performed adequately. The end-effector follows the desired trajectory, as represented by a straight line on the above figures. When a criterion is optimized, manipulability is maintained up to a certain level. Nevertheless, in the case of w optimization, local deteriorations are observed; these correspond to graining points in the platform trajectories. In the case of w_d optimization, local degradation does not appear. Moreover, since w_d takes task direction into account, the platform advances normally. The arm is more heavily constrained by w_d, which adds a supplementary condition on the task direction. The platform seeks to replace the arm more quickly in those configurations better adapted to following the direction imposed by the task in progress.

This more natural behavior offers the advantage of not disorienting the individual, an important feature in assistive robotics, which calls for the robot to work in close cooperation with the disabled host.

8 CONCLUSION

The purpose of this paper is to utilize system redundancy in order to maximize arm manipulability. With arm manipulability measures serving as performance criteria within a real-time control scheme, task execution has been accomplished with preferred arm configurations, as measured by manipulability. The platform trajectories obtained however contain graining points, especially when the system is poorly-oriented with respect to the operational task. The platform moves in reverse gear for the most part of task execution. We have proposed a new measure that associates information on task direction with a manipulation capability measure. As shown during our work, use of this proposed measure as a criterion allows performing the imposed task with human-like smooth movements and acceptable configurations from a manipulability perspective. The number of platform trajectory graining points is thus reduced and, for the most part, the platform is advancing.

Our latest work is focusing on the inclusion of obstacle avoidance in the control scheme in order to improve coordination between the two subsystems. Another work relates to the development of a control strategy for seizure. This strategy takes into account both of human-machine cooperation and the presence of obstacles in the environment.

REFERENCES

P. Baerlocher, “Inverse kinematics techniques for the interactive posture control of articulated figures,” PhD thesis, Lausanne, EPFL 2001.

B. Bayle, J.Y. Fourquet, M. Renaud, “Manipulability Analysis for Mobile Manipulators,” In ICRA’2001, Seoul, South Korea, pp. 1251-1256, May 2001.

B. Bayle, J. Y. Fourquet, M. Renaud. Using Manipulability with Nonholonomic Mobile Manipulators, 3rd International Conference on Field and Service Robotics (FSR'2001), Helsinki (Finlande), 11-13 Juin 2001, pp.343-348

M. Busnel, R. Gelin and B. Lesigne, “Evaluation of a robotized MASTER/RAID workstation at home: Protocol and first results”, Proc. ICORR 2001, Vol. 9, pp. 299-305, 2001.

G. Campion, G. Bastin and B. D’Andréa-Novel, “Structural proprieties and classification of kinematic and dynamic models of wheeled mobile robots,” IEEE Transaction on Robotics and Automation, Vol. 12, no. 1, pp. 47-62, February 1996.

P. Dario, E. Guglielmelli, B. Allotta, “MOVAID: a personal robot in everyday life of disabled and elderly people,” Technology and Disability Journal, no 10, IOS Press, 1999, pp. 77-93.

H. G. Evers, E. Beugels and G. Peters, “MANUS toward new decade”, Proc. ICORR 2001, Vol. 9, pp. 155-161, 2001.

P. Hoppenot, E. Colle, “Mobile robot command by man-machine co- operation - Application to disabled and elderly people assistance,” Journal of Intelligent and Robotic Systems, Vol. 34, no 3, pp 235-252, July 2002.

S. Kang, K. Komoriya, K. Yokoi, T. Koutoku, K. Tanie, “Utilization of Inertial Effect in Damping-based Posture Control of Mobile Manipulator,” International Conference on Robotic and Automation, pp. 1277-1282, Seoul, South Korea, May 2001.

O. Khatib, “Inertial properties in robotic manipulation: an object-level framework,” Int J. Robotics Research, Vol. 13, No. 1, pp. 19-36, 1995.

H. Kwee, C.A. Stanger, “The Manus robot arm”, Rehabilitation Robotics News letter, Vol. 5, No 2, 1993.

K. Nagatani, T. Hirayama, A. Gofuku, Y. Tanaka, “Motion planning for Mobile Manipulator with keeping Manipulability,” IROS 2002, , pp 1663-1668, Lausane, Switzerland, October 2002.

Y. Nakamura, “Advanced robotics, redundancy and optimization,” Addison Wesley Publishing, 1991.

J. K. Salisbury and J.J. Craig, “Articulated hands: Force Control and Kinematic Issues,” Intl. J. Robotics Research, Vol. 1, no. 1, pp. 4-17, 1982.

L. Sciavicco and B. Siciliano, “Modeling and control of robot manipulators,” The McGraw-Hill companies, Inc., 1996.

H. Seraji, “An on-line approach to coordinated mobility and manipulation,” In ICRA'1993, Atlanta, USA, May 1993, pp. 28-35.

D.E Whitney, “Resolved Motion Rate Control of Manipulators and Human Prosthetics,” IEEE Trans on Man Machine Systems, Vol 10, pp. 47-53, 1969.

Y. Yamamoto and X. Yun, “Coordinating locomotion and manipulation of mobile manipulator,” Recent Trends in Mobile Robots Zheng Y. Ed., 1987.

Y. Yamamoto and X. Yun, “Unified analysis an mobility and manipulability of mobile manipulators,” IEEE Int. Conf. Robotics and Automation, Detroit, pp. 1200-1206, USA, 1999.

T. Yoshikawa, “Manipulability of Robotic Mechanisms,” International Journal of Robotics Research, 1985, Vol. 4, no. 2, pp. 3-9.

Yoshikawa, T.: Foundation of robotics: Analysis and control, The MIT Press, 1990.

T. Yoshikawa, “Analysis and control of Robot manipulators with redundancy,” In M. Brady & R. Paul, editors, Robotics Research: The First International Symposium, MIT Press, pp. 735-747, 1984.

H.F.M. Van der Loos, “VA/Stanford Rehabilitation Robotics Research and Development Program: Lessons Learned in the Application of Robotics Technology to the Field of Rehabilitation,” IEEE Trans. Pn Rehabilitation Engineering, Vol. 3, n°1, pp. 46-55, March 1995.